

# The Inactivating Factor of Glutamine Synthetase IF17 Is an Intrinsically Disordered Protein, Which Folds upon Binding to Its Target

Lorena Saelices,<sup>†,⊥</sup> Carla V. Galmozzi,<sup>†</sup> Francisco J. Florencio,<sup>†</sup> M. Isabel Muro-Pastor,<sup>\*,†</sup> and José L. Neira<sup>\*,‡,§,⊥</sup>

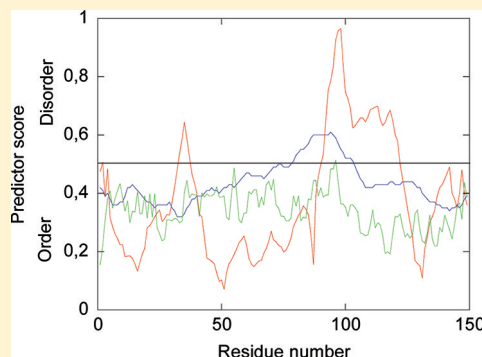
<sup>†</sup>Instituto de Bioquímica Vegetal y Fotosíntesis, CSIC-Universidad de Sevilla, Seville, Spain

<sup>‡</sup>Instituto de Biología Molecular y Celular, Universidad Miguel Hernández, Elche (Alicante), Spain

<sup>§</sup>Instituto de Biocomputación y Física de Sistemas Complejos, Zaragoza, Spain

## Supporting Information

**ABSTRACT:** In cyanobacteria, ammonium is incorporated into carbon skeletons by the sequential action of glutamine synthetase and glutamate synthase (GOGAT). The activity of *Synechocystis* sp. PCC 6803 glutamine synthetase type I (GS) is controlled by a post-transcriptional process involving protein–protein interactions with two inactivating factors: the 65-residue-long protein (IF7) and the 149-residue-long one (IF17). The sequence of the C terminus of IF17 is similar to IF7; IF7 is an intrinsically disordered protein (IDP). In this work, we study the structural propensities and affinity for GS of IF17 and a chimera protein, IF17N/IF7 (constructed by fusing the first 82 residues of IF17 with the whole IF7) by fluorescence, CD, and NMR. IF17 and IF17N/IF7 are IDPs with residual non-hydrogen-bonded structure, probably formed by  $\alpha$ -helical, turn-like, and PPII conformations; several theoretical predictions support these experimental findings. IF17 seems to fold upon binding to GS, as suggested by CD thermal denaturations and steady-state far-UV spectra. The apparent affinity of IF17 for GS, as measured by fluorescence, is slightly smaller ( $K_D \sim 1 \mu\text{M}$ ) than that measured for IF7 ( $\sim 0.3 \mu\text{M}$ ). The  $K_D$ s determined by CD are similar to those measured by fluorescence, but slightly larger, suggesting possible conformational rearrangements in the IFs and/or GS upon binding. Further, the results with IF17N/IF7 suggest that (i) binding of IF17 to the GS is modulated not only by its C-terminal region but also by its N-terminus and (ii) there are weakly structured (that is, “fuzzy”) complexes in the ternary GS–IF system.



Ammonium assimilation is the process by which this nitrogen form is incorporated into carbon skeletons. This process takes place in the majority of microorganisms by the sequential action of glutamine synthetase and glutamate synthase (GOGAT). Glutamine synthetase catalyzes the ATP-dependent amidation of glutamic acid to yield glutamine. GOGAT is able to transfer the amide group from glutamine to 2-oxoglutarate, yielding two molecules of glutamic acid. This protein network (the so-called GS–GOGAT cycle) is therefore the connecting step between carbon and nitrogen metabolism. In fact, activity and synthesis of glutamine synthetase are exquisitely tuned by those sources: in the presence of high levels of carbon metabolites, nitrogen deficiency leads to high levels of glutamine synthetase activity, and conversely, when nitrogen is abundant, glutamine synthetase activity is down-regulated.<sup>1,2</sup>

In cyanobacteria, GS type I (GS) is modulated at the transcriptional and post-transcriptional levels, according to the nitrogen and carbon supplies.<sup>3</sup> The classical feedback inhibition, or covalent modification by adenylation of GS observed in other bacteria,<sup>4</sup> does not occur in cyanobacteria.

However, there is a post-translational regulation mechanism involving protein–protein interactions:<sup>5–7</sup> a 65-residue-long protein named IF7 and a 149-residue-long one named IF17. Analysis of mutant strains devoid of IF7, IF17, or both have shown that each of these proteins contributes to GS inactivation *in vivo*; interestingly enough, a maximal level of inactivation has been observed when both proteins are present.<sup>5</sup> In the presence of ammonium, IF7 and IF17 are expressed and GS is inactivated; on the other hand, removal of ammonium leads to a degradation of IF7 and IF17.<sup>8</sup> Moreover, recombinant IF7 and IF17 inactivate GS *in vitro*, indicating that both factors can interact with GS without additional modifications.<sup>5</sup> In addition, the expression of both proteins is modulated by NtcA, the main factor responsible for nitrogen control in cyanobacteria.<sup>3,9,10</sup>

ORFs homologous to the IF7 and IF17 encoding genes can be identified in several cyanobacterial genomes (ref 3 and

**Received:** June 16, 2011

**Revised:** October 10, 2011

**Published:** October 12, 2011



references therein); in fact, sequence comparison suggests two groups of IFs: those similar to IF7 and those to IF17 from *Synechocystis*. Most cyanobacterial strains have IF7-like inactivating factors (65–68 amino acids), whereas *Thermosynechococcus elongatus* harbors IF17-like inactivating factors. There is a large sequence similarity between the C terminus of IF17 and the full IF7 of *Synechocystis*, which suggests that both polypeptide regions may be involved in the interaction with GS, and they are therefore responsible for the inactivating activity.<sup>3</sup> Furthermore, IF7 and IF17 from *Synechocystis* have different proteolytic stabilities *in vivo*,<sup>8</sup> and it has been suggested that the N-terminal region of IF17 could be responsible for the different stabilities.<sup>8</sup> In fact, a chimera construction of the first 82 residues of IF17 from *Synechocystis* and the IF7 from *Anabaena* sp. PCC7120 (IF7A) showed a larger stability than the wild-type IF7A but less inactivation of GS than IF7A, probably pinpointing the specificity of the IF–GS inactivation.<sup>7</sup>

We have shown that IF7 from *Synechocystis* is an IDP.<sup>11</sup> In this work, we report the structural preferences and conformational stability of IF17 from *Synechocystis* sp. PCC 6803. Furthermore, to address the importance of the N-terminus of IF17 in GS binding, we used a chimera protein (IF17N/IF7) formed by the first 82 residues of the IF17 fused to IF7. We studied the affinity of IF17 for GS, in the absence and in the presence of IF7, and the interaction of GS with IF17N/IF7. Our results show that both IF17 or IF17N/IF7 are IDPs, and thus, the 82-residue-long N-terminus of IF17 does not help to stabilize any structure in IF7, and it does not increase the conformational stability of IF17. Furthermore, the GS affinity of IF17, as determined by fluorescence, is slightly smaller than that of isolated IF7.<sup>11</sup> The  $K_D$ s determined by CD are similar to those measured by fluorescence, but slightly larger, suggesting conformational rearrangements in the IFs and/or GS upon binding. Finally, the results with the chimera protein suggest the presence of weakly structured complexes in the GS–IF system.

## EXPERIMENTAL PROCEDURES

**Materials.** Deuterium oxide was obtained from Apollo Scientific (Stockport, UK), and sodium trimethylsilyl-[2,2,3,3-<sup>2</sup>H<sub>4</sub>]propionate, TSP, was from Sigma (St. Louis, MO). Ultrapure GdmCl and urea were from MP Biomedicals (Solon, OH). Dialysis tubing, with a molecular weight cutoff of 3500 Da, was from Spectrapor (Spectrum Laboratories, Japan). Amicon centrifugal devices with a molecular weight cutoff of 3500 Da were from Millipore (Millipore, Spain). Standard suppliers were used for all other chemicals. Water was deionized and purified on a Millipore system.

**Protein Expression and Purification.** The recombinant GS, IF17, and IF7 proteins were expressed and purified as described.<sup>5,7</sup> The IF17N/IF7 protein was designed in a manner similar to that described for the chimera containing the N-terminal region of IF17 from *Synechocystis* fused to IF7A;<sup>7</sup> purification of IF17N/IF7 was similar to the protocol used for IF17.<sup>7</sup> Protein stocks were run in SDS-PAGE gels and found to be >97% pure. Protein concentrations were determined from the absorbance of individual amino acids.<sup>12</sup>

**Fluorescence.** Spectra were collected on a Cary Eclipse spectrofluorometer (Varian, Palo Alto, CA) interfaced with a Peltier system. A 1 cm-path-length quartz cell (Hellma) was used. Experiments were carried out at 25 °C in phosphate buffer at pH 7.0 (10 mM).

**a. Steady State Fluorescence Measurements.** Spectra of isolated IF17 and IF17N/IF7 were acquired by excitation at 280 or 295 nm; the emission was collected between 300 and 400 nm. The excitation and emission slits were set to 5 nm, and the response was 1 nm.

Binding experiments of the IFs to GS were carried out as described.<sup>11</sup> Briefly, increasing amounts of the corresponding IF, in the range 0.25–4  $\mu$ M, were added to a solution containing 1.5  $\mu$ M (in protomer units) of GS, in 10 mM phosphate buffer (pH 7.0); the fluorescence was measured at 25 °C after preparing the samples. The apparent dissociation constants of the GS-IF complexes,  $K_D$ , were calculated by fitting the fluorescence changes in intensity, or in the average energy  $\langle\lambda\rangle$ ,<sup>13</sup> versus the concentration of added protein to

$$F_{\text{meas}} = F + \Delta F_{\text{max}} \left( \frac{[\text{protein}] + [\text{GS}] + K_D}{([\text{protein}] + [\text{GS}] + K_D)^2 - 4[\text{GS}][\text{protein}]} \right)^{1/2} \quad (1)$$

where [protein] is the concentration of added protein (IF7, IF17, or IF17N/IF7), [GS] is the concentration of GS (in protomer units),  $F_{\text{meas}}$  is the measured fluorescence parameter at each concentration of added IF,  $\Delta F_{\text{max}}$  is half of the change in that parameter, when all GS is forming the complex, and  $F$  is the fluorescence parameter of the mixture of the complex formed by GS and an IF at the beginning of the titration (see below). Every titration experiment was repeated twice with new samples. It is interesting to note here that the use of [IF17] or [IF7] 3–4-fold or more than the [GS] yielded sample precipitation in the binding experiments. These results agree with functional assays, since it has been shown that the complete inactivation of GS occurs at concentrations of IFs 4 times larger than the [GS].<sup>5</sup> Fitting to eq 1 was carried out with Kaleidagraph (Abelbeck software).

The following titrations were carried out: (i) measurement of the apparent  $K_D$  of GS-IF17 complex; (ii) measurement of the apparent  $K_D$  of IF17 for GS in the presence of 3.0  $\mu$ M IF7 (where all the IF7 binding sites of GS are saturated<sup>11</sup>); (iii) measurement of the apparent  $K_D$  of IF7 for GS in the presence of 3.0  $\mu$ M of IF17 (where all the IF17 binding sites of GS are saturated, see Results); and (iv) measurement of the apparent  $K_D$  of IF17N/IF7 for GS. The first two experiments were acquired by excitation at 295 nm, since IF17 has no tryptophans; the last two assays were carried out by excitation at 280 and 295 nm, and the corresponding contributions of the IFs to the reaction mixture were subtracted. As a control experiment, we also carried out a titration of IF7, similar to that described in ref 11.

**b. Thermal Denaturations.** Spectra were acquired by excitation at 280 or 295 nm; the emission fluorescence was collected at 315, 335, and 350 nm. The excitation and emission slits were set to 5 nm; the response was 1 nm, and the scan rate was 60 °C/h, with an average data point of 1 s. The experiments were repeated twice with new samples. All the thermal denaturations involving the GS or GS–IFs complexes were irreversible. The thermal denaturation midpoints ( $T_m$ s) of the sigmoidal curves were obtained by using Kaleidagraph (Abelbeck software) as described (Table 1).<sup>13</sup>

**Circular Dichroism.** Spectra were collected on a Jasco J810 (Japan) spectropolarimeter connected to a Peltier unit. The instrument was periodically calibrated with (+)-10-camphorsulfonic acid. Spectra were acquired at 25 °C in

**Table 1.**  $T_m$ s (in °C) for the Protein GS and Its Complexes with the IFs<sup>a</sup>

protein/complex	CD	fluorescence
GS	66.2 ± 0.2	67.2 ± 0.5
GS (pH 8.5)	61.4 ± 0.5	<i>b</i>
GS + IF7	68.9 ± 0.1	68.60 ± 0.08
GS + IF17	44.4 ± 0.2 (1st transition) 70.3 ± 0.8 (2nd transition)	72.3 ± 0.5
GS + IF17 (pH 8.5)	68.2 ± 0.3	<i>b</i>
GS+ IF7 + IF17	44.7 ± 0.8 (1st transition) 71.3 ± 0.6 (2nd transition)	73.3 ± 0.5
GS + IF17N/IF7	43.3 ± 0.9 (1st transition) 68.2 ± 0.8 (2nd transition)	68.6 ± 0.8

<sup>a</sup>The errors are the standard deviations from three measurements with new samples. All the measurements were carried out at pH 7.0 (10 mM phosphate buffer), unless otherwise stated. GS concentration, in the CD and fluorescence measurements, was 1.5  $\mu$ M (in protomer units), and the concentration of IFs were typically 3  $\mu$ M; the samples were prepared fresh. The  $T_m$ s were obtained as described.<sup>13</sup> All the thermal denaturations were irreversible. <sup>b</sup>Not determined.

phosphate buffer at pH 7.0 (10 mM). Appropriate blank solutions were subtracted.

**a. Steady State Measurements.** Spectra of IF17, IF7, IF17N/IF7, and GS in the far-UV CD were acquired with a response time of 2 s, and averaged over 4 scans, with a scan speed of 50 nm/min. The step resolution was 0.2 nm, and the bandwidth was 1 nm. Molar ellipticity was obtained as described.<sup>11</sup> The GS concentration was 1.5  $\mu$ M of protomer, and that of the IFs was 3  $\mu$ M in the experiments aimed to detect complex formation. The path length cell was 0.1 cm. Every experiment was repeated three times with new samples.

The path length was 0.5 cm in the near-UV CD experiments aimed to characterize IF17 and IF17N/IF7, with a protein concentration of 60–70  $\mu$ M. Experiments were averaged over 6 scans, with a response time of 8 s and a bandwidth of 1 nm. Every experiment was repeated three times with new samples.

For the experiments at different pHs of IF17, the salts and acids used in buffer preparation were pH 2.0–3.0, phosphoric acid; pH 3.0–4.0, formic acid; pH 4.0–5.5, acetic acid; pH 6.0–7.0,  $\text{NaH}_2\text{PO}_4$ ; pH 7.5–9.0, Tris acid; and pH 9.5–11.0,  $\text{Na}_2\text{CO}_3$ . The pH was measured with an ultrathin Aldrich electrode in a Radiometer (Copenhagen) pH-meter. The samples were prepared the day before and left overnight at 25 °C to equilibrate. The pH was measured after completion of the experiments, and essentially no differences were observed with those pHs calculated from the buffer stocks. Final buffer concentration was 10 mM in all cases. The pH titration was repeated twice with new samples.

In the GdmCl denaturations, far-UV CD spectra of either IF17 or IF17N/IF7 were acquired at a scan speed of 50 nm/min, and four scans were recorded and averaged at 25 °C. The response time was 2 s. The cell path length was 0.1 cm, with a protein concentration of 10  $\mu$ M. Spectra were corrected by subtracting the corresponding baseline. The chemical denaturations were fully reversible, and they were repeated three times with new samples.

We also carried out binding titrations of GS with both IFs by using the same experimental setup described above. To allow for a comparison with the fluorescence results, we took

advantage of the fact that GS is a homoligomeric protein, and then concentrations as low as 1.5  $\mu$ M of GS were used in the CD binding titrations. After careful observation of the spectra at the different IF concentrations used, the best wavelengths to monitor the changes upon GS binding were chosen between 222 and 210 nm. The following titrations were carried out: (i) measurement of the apparent  $K_D$  of GS-IF17 complex; (ii) measurement of the apparent  $K_D$  of GS-IF7 complex; (iii) measurement of the apparent  $K_D$  of IF17 for GS in the presence of 3.0  $\mu$ M IF7 (where all the IF7-binding sites of GS are saturated<sup>11</sup>); and (iv) measurement of the apparent  $K_D$  of IF7 for GS in the presence of 3.0  $\mu$ M IF17 (where all the IF17-binding sites of GS are saturated, see below). In all cases, appropriate blank corrections (IF7 or IF17) were subtracted from the spectra of the resulting complex at the different IF concentrations; the blank solutions contained the buffer and the corresponding amount of the IF protein, but they did not contain GS. This subtraction of spectra make that the experimental points (the value of the ellipticity at different wavelengths) be more scattered than in the fluorescence measurements (Figure 3 of Supporting Information). The binding CD curves were fitted to eq 1 by using Kaleidagraph (Abelbeck software).

In the four CD titrations, the measured apparent constants were close to those determined by fluorescence (Table 2), and then, we did not carry out additional titration experiments with the chimera protein, due to the large amounts of IF17N/IF7 being used (in the samples for complex formation and in the corresponding blanks).

**b. Thermal Denaturations.** Thermal denaturations were carried out by following the changes at 222 nm, at 60 °C/h, with a response time of 8 s. All the denaturations involving GS were irreversible. The denaturations of isolated IF17 and IF17N/IF7 were reversible: samples were transparent, and no precipitation was observed after the reheating; furthermore, the steady-state spectra for each protein after heating and cooling at 25 °C were identical to those obtained before heating. In addition, the monitored voltages of the photomultiplier during the thermal scans did not show any sigmoidal behaviors, but rather they increased linearly as the temperature was raised; this trend in the voltage of the lamp is an indication of reversibility during the thermal denaturations.<sup>14</sup> Finally, we also carried out a thermal forward–backward scan with an IF17 sample, and the two curves were superimposable (data not shown), suggesting lack of hysteresis behavior. The possibility of drifting of the CD spectropolarimeter was tested by running two samples containing only buffer, before and after the thermal experiments. No difference was observed between the scans. The experiments were repeated twice with new samples. Fittings of the sigmoidal curves were carried out as described<sup>13</sup> by using Kaleidagraph (Abelbeck software).

We also carried out thermal denaturation experiments at growing concentrations of IF17, with a constant concentration of GS (1.5  $\mu$ M), trying to determine the origin of the low thermal transition observed in GS in the presence of IF17 (see below). In addition, several thermal scans were acquired up to a temperature of 57 °C (larger than the  $T_m$  of the first transition observed in samples containing IF17, see Figure 3B of Supporting Information), and then, the samples were cooled and rescanned to see if the first thermal transition was observed. In all cases, the first transition was not observed in the reheating scan.



Table 2. Apparent  $K_D$ s for GS–IFs Complexes<sup>a</sup>

complex	$K_D$ ( $\mu$ M) (CD)	$K_D$ ( $\mu$ M) (fluorescence)	stoichiometry ([IFs]/[GS]) <sup>b</sup> (fluorescence)
GS + IF7 <sup>c</sup>	4.3 $\pm$ 2.7	0.35 $\pm$ 0.09	0.5 $\pm$ 0.2
GS + IF17	2.2 $\pm$ 1.5	1.3 $\pm$ 0.6	0.5 $\pm$ 0.3
(GS + IF7) + IF17 <sup>d</sup>	3.2 $\pm$ 1.8	0.3 $\pm$ 0.1	1 $\pm$ 0.4
(GS+ IF17) + IF7 <sup>e</sup>	1.8 $\pm$ 0.9	0.8 $\pm$ 0.3	1 $\pm$ 0.2
GS + IF17N/ IF7 <sup>f</sup>	g	0.8 $\pm$ 0.5	1 $\pm$ 0.5

<sup>a</sup>The errors in the fluorescence measurements are the standard deviations from three determinations at different wavelengths (315, 335, and 350 nm), unless it is stated. All the measurements were carried out at pH 7.0 (10 mM phosphate buffer), at 25 °C. GS protein concentration was 1.5  $\mu$ M of protomer, either in the CD or fluorescence experiments. Because of the almost lack of IF7 signal in the far-UV CD at the concentrations used, the blank spectra had a larger signal-to-noise ratio than those obtained when IF17 was varied, and then the resulting curves had a poorer fitting. <sup>b</sup>Errors in the stoichiometry, as obtained by fluorescence, were determined from the error propagation.<sup>53</sup> A plot of the difference between the measured fluorescence of the complex, and that expected from the contribution of the individual GS and IF proteins, versus the ratio [titrating IF protein]/[GS protomer] provides two straight lines whose intersection, in the  $x$ -axis coordinate, gives the complex stoichiometry. The errors in the intersection of the two straight lines were determined from the errors in their slopes and in their  $y$ -axis intercepts. The stoichiometry was not determined from CD measurements due to the large error in the slopes and  $y$ -axis intercepts of the straight lines. <sup>c</sup>The  $K_D$  from fluorescence is similar to that previously reported,<sup>11</sup> and the stoichiometry is determined from the values obtained in the fluorescence titration in this work. The value of the apparent  $K_D$  by CD was determined from data in this work. <sup>d</sup>The IF17 concentration was varied during the titration (either followed by CD or fluorescence). The concentration of IF7 in the mixture was kept constant and equal to 3  $\mu$ M. <sup>e</sup>The IF7 concentration was varied during the titration (either followed by CD or fluorescence). The concentration of IF17 in the mixture was kept constant and equal to 3  $\mu$ M. <sup>f</sup>The reported  $K_D$  is the mean value of the measurements from the average energies<sup>13</sup> at 280 and 295 nm. The error is the standard deviation of the fitting of the  $\langle\lambda\rangle$  at the two wavelengths. The use of the fluorescence intensities at several wavelengths in this titration led to unreliable values. <sup>g</sup>Not determined.

**NMR Spectroscopy.** The NMR experiments were acquired at 25 °C on a Bruker Avance DRX-500 spectrometer (Bruker GmbH, Germany), equipped with a triple resonance probe and  $z$ -pulse field gradients. Processing of spectra was carried out with the XWINNMR software. All experiments were carried out at pH 7.0, 10 mM phosphate buffer, and with a protein concentration of 100  $\mu$ M. Samples were concentrated by using Amicon centrifugal devices.

**a. 1D NMR Experiments.** TSP was used as the external chemical shift reference in the 1D NMR spectra. Water was suppressed with the WATERGATE sequence.<sup>15</sup> Usually, 512 scans were acquired with a spectral width of 12 ppm, with 16K data points in the time domain. The data matrix was zero-filled to 32K during processing. Experiments were carried out at pH 5.9.

Exchange experiments were carried out by dissolving in D<sub>2</sub>O, at pH 5.9 (no corrected by isotope effects), a lyophilized IF17 sample to yield a final concentration of 80  $\mu$ M. The sample was centrifuged in a cold room to remove any insoluble material, transferred to the NMR tube and then to the magnet (the

whole process took approximately 5–10 min). Experiments were acquired at 20 °C.

**b. Translational Diffusion NMR Experiments (DOSY).** Translational self-diffusion measurements were performed with the pulsed-gradient spin-echo sequence. The following relationship exists between the translational self-diffusion constant,  $D$ , and the delays during acquisition:<sup>13</sup>  $I/I_0 = -\exp[D\gamma_H^2\delta^2G^2(\Delta - \delta/3 - \tau/2)]$ , where  $I$  is the measured peak intensity of a particular (or a group of) resonance(s) at any gradient strength,  $I_0$  is the maximum peak intensity of the same resonance(s) at the smallest gradient strength (that is, at 2% of the total power of the gradient coil),  $D$  is the translational self-diffusion constant (in cm<sup>2</sup> s<sup>-1</sup>),  $\delta$  is the duration (in s) of the gradient,  $G$  is the gradient strength (in T cm<sup>-1</sup>),  $\Delta$  is the time (in s) between the gradients,  $\gamma_H$  is the gyromagnetic constant of the proton, and  $\tau$  is the recovery delay between the bipolar gradients (100  $\mu$ s in our experiments). The gradient strength ( $G$ ) was varied in 16 linear steps between 2 and 95% of the total power of the gradient coil of the probe. Data are plotted as  $I/I_0$  versus  $G^2$ , and the exponential factor of the resulting curve is  $D\gamma_H^2\delta^2(\Delta - \delta/3 - \tau/2)$ , from where  $D$  can be easily obtained. The duration of the gradient ( $\delta$ ) was varied between 1.8 and 2.5 ms, and the time between both gradients ( $\Delta$ ) was changed from 100 to 150 ms. The methyl groups between 0.8 and 1 ppm were used for integration. The gradient strength was calibrated by using the value of  $D$  for the residual proton water line in a sample containing 100% D<sub>2</sub>O in a 5 mm tube.<sup>13</sup> The hydrodynamic radius,  $R$ , was obtained by assuming that the  $R$  of dioxane is 2.12 Å.<sup>16</sup> The DOSY experiment was repeated twice.

**Bioinformatic Analysis of Amino Acid Sequences of IF17 and IF17N/IF7.** The sequences of IF17 and IF17N/IF7 were submitted to the PONDR server, and analyses were performed using the neural network predictor VL-XT and CDF<sup>17,18</sup> (access to PONDR was provided by Molecular Kinetics). We also used the IUPRED,<sup>19,20</sup> RONN,<sup>21</sup> and Foldindex.<sup>22</sup> The ANCHOR server was used to predict the putative binding sites of IF7, IF17, and IF17N/IF7.<sup>23,24</sup>

## RESULTS

**The IF17 Protein Is Disordered in Solution.** To characterize the structure, stability, and conformational propensities of IF17 in aqueous solution, we combined experimental and theoretical approaches.

**a. Spectroscopic Characterization and Conformational Stability.** Within the experimental approach, we used fluorescence, CD, and NMR spectroscopies.

**Fluorescence.** We have used fluorescence spectroscopy to map any change in the tertiary structure of the protein.<sup>25</sup> Since IF17 has no tryptophan residues, and it contains eight tyrosines, the fluorescence spectrum had a maximum wavelength at 306 nm, which was unaltered at the pHs explored. The thermal denaturations of IF17 showed a linear decrease in the fluorescence emission as the temperature was increased (data not shown).

**Circular Dichroism.** **a. Far-UV CD.** We used far-UV CD in the analysis of the structure and conformational stability of IF17 as a spectroscopic probe that is sensitive to secondary structure.<sup>26,27</sup> The CD spectrum of IF17, at 25 °C and physiological pH, showed a minimum negative ellipticity at ~200 nm and a negative shoulder around 222 nm (Figure 1). These results suggest an unfolded protein with a small fraction of  $\alpha$ -helix, turn-like, or PPII structures,<sup>28</sup> although the presence

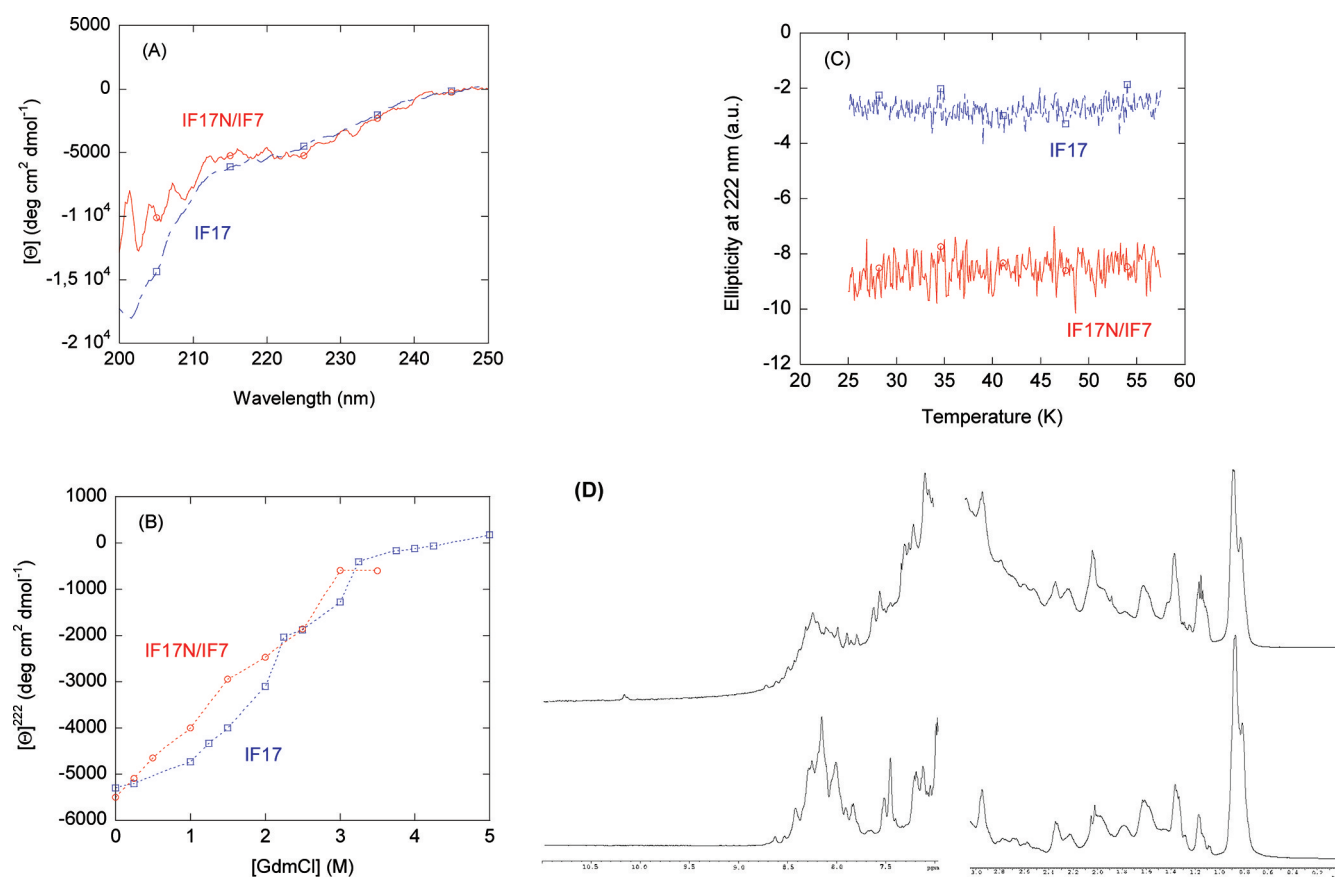


**Figure 1.** Spectroscopic features and conformational stabilities of IF17 and IF17N/IF7. (A) Far-UV spectra of IF17 and IF17N/IF7. (B) GdmCl denaturations followed by the changes in the ellipticity at 222 nm in the far-UV CD spectra of IF17 (blue squares) and IF17N/IF7 (red circles). The lines through the data have been drawn to guide the eye, and they do not represent any fitting curves. (C) Thermal denaturations of IF17 and IF17N/IF7 followed by the changes in the ellipticity at 222 nm (the scale on the y-axis is arbitrary, and the thermograms have been scaled up for the reader's sake). (D) The amide and aromatic (left) and methyl (right) regions of the IF17N/IF7 (top) and IF17 (bottom) 1D NMR spectra. Experiments were acquired at pH 7.0 (phosphate buffer, 10 mM) and 25 °C.

of aromatic signals, which also absorb at 222 nm, cannot be ruled out.<sup>27</sup> We can estimate the helical or turn-like populations from the molar ellipticity at 222 nm ( $-5300 \text{ deg cm}^2 \text{ dmol}^{-1}$ ),<sup>11</sup> leading to a 14%. Deconvolution of the far-UV CD spectrum by using the DICHROWEB server<sup>29,30</sup> leads to a 61% of unordered structure and a 29% of turn-like conformations, with no helical conformations; we used in DICHROWEB the reference data 6, which contains the spectra of several denatured proteins and hence produces a more accurate prediction when the protein contains disordered structure. There is a discrepancy between the value determined by DICHROWEB and that from the approach using the ellipticity at 222 nm. This difference must be due to the fact that at 222 nm the  $\beta$ -sheet could also absorb or, as stated above, aromatic residues; furthermore, the difference could be also due to the deconvolution algorithms used in DICHROWEB.<sup>29,30</sup>

**b. Chemical and Thermal Denaturations.** To investigate the stability of the residual structure in IF17, we carried out chemical (GdmCl and urea) and thermal denaturations.

The ellipticity at 222 nm decreased (in absolute value) gradually as the concentration of GdmCl (or urea) was increased (Figure 1B), indicating that the unfolding was a noncooperative process. It could be thought that the chemical denaturation of IF17 resembled a sigmoidal-like shape, since an apparent slope transition and an unfolding baseline seem to be observed (Figure 1B, red squares); however, attempts to fit

these data to a two-state model failed due to the large slope imposed to the putative native baseline and yielded chemical denaturation midpoints with fitting errors larger than 100%. Furthermore, a similar behavior (that is, detection of a sloping transition and unfolding baseline regions of a sigmoidal curve, but absence of a native baseline) has been observed in other IDPs during their chemical denaturations (refs 31–34 and other references in refs 31 and 33), in thermal denaturations of IDPs,<sup>32,35</sup> and in the chemical denaturation of IF7;<sup>11</sup> it seems that the sigmoidal-like shapes are associated with the presence of some residual structure in IDPs having the sizes of molten or premolten globules.<sup>31,33</sup> The ellipticity of IF17 showed a linear behavior as the temperature was raised (Figure 1C), in agreement with the fluorescence thermal denaturations (see above). This behavior is commonly observed among IDPs, and it is explained as due to a redistribution of the random coil involving a loss of PPII and/or helical conformations.<sup>35</sup>

**c. pH Titrations.** At pH 8.5, the binding between GS and IF17 is weakened as shown by gel-shift assays,<sup>8</sup> suggesting possible conformational changes in IF17, which could hamper the interaction. To test this hypothesis, we carried out pH titrations of IF17. The shape of the spectrum of IF17 did not change in the pH range explored, and the ellipticity at 222 nm remained constant (Figure 1 of Supporting Information), except at pH > 10, probably due to basic denaturation and/or titration of tyrosine residues. Thus, the weakening of the GS-

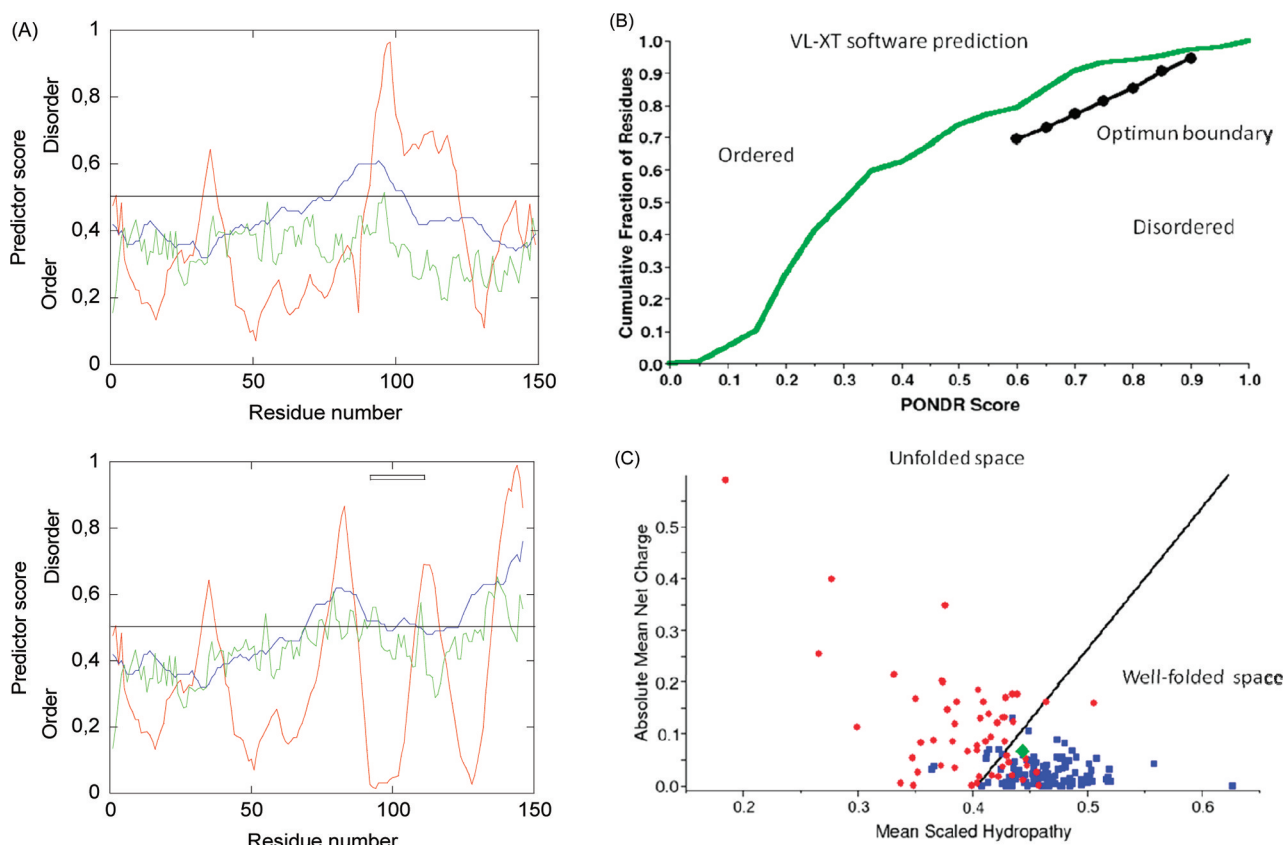


**Figure 2.** *In silico* analysis of IF17 and IF17N/IF7 sequences. (A) Predictions of unstructured regions of IF17 (top) and IF17N/IF7 (bottom) sequences with the use of VL-XT (red), RONN (blue), and IUPred (green) predictors. The results of ANCHOR web server for IF17N/IF7 are indicated as a black bar comprising the residues involved at the top of the panel; ANCHOR did not predict any binding region for IF17. The line indicates the 0.5 cutoff limit for the three predictors. (B) PONDR prediction of unstructured regions of IF17 with the use of the CDF predictor (cumulative distribution function). CDF predictor of IF17 falls above the optimum boundary (black line), indicating a well-folded polypeptide chain. (C) Charge hydrophobicity phase space separation between ordered proteins (filled blue squares) and natively unfolded proteins (filled red circles); the IF17 (green diamond) falls within the well-folded (ordered) space. Panels B and C were directly obtained from the PONDR software.

IF17 binding at pH 8.5 is not due to changes in the structure of IF17.

**d. Near-UV CD.** We used near-UV CD to detect possible changes in the asymmetric environment of aromatic residues.<sup>26,27</sup> The near-UV of IF17 was very weak, and there were no intense bands. There are two possible explanations for this behavior. First, the absence of a near-UV signal could be due to the lack of a rigid asymmetric environment for the aromatic residues. And second, it could be due to the relatively low content of aromatic residues (eight tyrosines, four phenylalanines, and one histidine; that is, 13 out of 149 residues). We favor the first explanation due to the experimental findings described above and to the following experiments.

**NMR Spectroscopy.** *a. 1D NMR.* NMR can give information about the general fold of a polypeptide chain in solution at the residue level.<sup>36</sup> The 1D NMR spectrum of IF17 at 25 °C showed a poor chemical shift dispersion: the amide, the aromatic, and the methyl protons (Figure 1D) were clustered in those regions expected for random-coil proteins:<sup>36</sup> namely, between 8.0 and 8.7 ppm (for the amide signals), between 6.8 and 7.3 ppm (for the aromatic protons), and between 0.8 and 1.0 ppm (for the methyl groups). The line widths of amide protons were not significantly broader than those of proteins with similar size (Figure 1D, left side); in fact, 1D NMR experiments at 50  $\mu$ M did not show any change in

the line widths, when compared to the spectra at 100  $\mu$ M. These results suggest that the protein is a monomer under these conditions.

We also carried out hydrogen-exchange experiments. After 10 min at 20 °C at pH 5.9, all the amide protons of IF17 in the 1D NMR spectrum were exchanged, suggesting the absence of hydrogen bonds.

**b. DOSY-NMR.** To get insight into the hydrodynamic properties of IF17, we first tried analytical size exclusion chromatography with a Superdex 16/60 HR column (GE Healthcare). However, at the different pHs explored (pH 5, 7, and 9), IF17 eluted at volumes larger than the column bed volume ( $\sim$ 19 mL), suggesting protein–column interactions. Therefore, we decided to determine the  $R$ , and the protein oligomerization state of the molecule, from the measurements of the translational diffusion coefficient ( $D$ ), by DOSY-NMR experiments. The measured  $D$  was  $(7.5 \pm 0.1) \times 10^{-7} \text{ cm}^2 \text{ s}^{-1}$ , which yields an  $R = 26 \pm 2 \text{ \AA}$  (with a dioxane  $D$  value of  $(9.3 \pm 0.1) \times 10^{-7} \text{ cm}^2 \text{ s}^{-1}$ ).

It is illustrative to compare the experimental value of the  $R$  with the theoretical estimations for folded and unfolded proteins. The theoretical value of the  $R$  for an unsolvated spherical molecule,  $R_t$ , is given by  $R_t = (3M\bar{V}/4N_A\pi)^{1/3}$ , where  $\bar{V}$  is the specific volume (0.736  $\text{cm}^3/\text{g}$  for IF17),  $N_A$  is Avogadro's number, and  $M$  is the molecular weight (16 679.9 Da for IF17). For a monomeric IF17, the above expression



leads to an  $R_g = 17.0$  Å (for a dimeric one is 21.3 Å), which is different to that measured experimentally (26.2 Å). On the other hand, the  $R$  for a well-folded protein is given by  $R = (4.75 \pm 1.11)N^{0.29 \pm 0.02}$ ,<sup>16</sup> where  $N$  is the number of residues. This expression yields a value of  $20 \pm 3$  Å for a monomeric IF17, which is similar to that obtained for a well-folded protein, with the use of Uversky equations:<sup>37</sup> 20.1 Å. The use of the equation for a premolten globule species<sup>37</sup> yields an  $R$  value of  $29 \pm 5$  Å, which is similar, within the experimental error, to the measured one. (The  $R$  value for a molten globule according to the same equations is  $22 \pm 8$  Å, which is also similar to the experimental value.) These findings suggest that IF17 is a monomer with a molten or premolten globule conformation.

We can calculate the theoretical  $R$  of an unfolded protein, with the same number of residues as IF17, by using Flory's scaling law:  $R = R_0 N^\nu$ , where  $R_0$  is a constant and  $\nu$  is a solvent-dependent scaling factor. The value of  $R_0$  and  $\nu$  change among the authors in the literature,<sup>16,38–40</sup> but for all the assayed pairs of values, the  $R$  for an unfolded IF17 ranges from 31 to 38 Å, similar to the value obtained by the Uversky equation ( $37 \text{ Å}^{37}$ ).

Taken together, these results indicate that the IF17 is more compact than a fully disordered polypeptide chain but is not a fully spherical well-folded globular protein. Furthermore, several findings suggest that IF17 is a monomer in aqueous solution. First, the far-UV CD spectra at two IF17 concentrations (10 and 20  $\mu\text{M}$ ) were identical (data not shown). Second, the NMR line widths of the spectra at two protein concentrations (50 and 100  $\mu\text{M}$ ) did not change. And finally, the size of IF17 is close to that of a monomeric premolten or molten globule-like species.

**b. Theoretical Analysis of the IF17 Sequence.** Results from the application of different theoretical predictors were puzzling. The VL-XT program predicts that most of the polypeptide chain is ordered: only residues Tyr33–Arg37 and Ala91–Val123 were disordered (Figure 2A, top panel, red line). Furthermore, the CDF analysis of PONDR predicts that IF17 is a well-folded protein (Figure 2B). The RONN server predicts that the only disordered patch comprises Ala79 to Arg103, and thus, it overlaps with the second region predicted by VL-XT (Figure 2A, top panel, blue line). The FoldIndex server indicates that the regions Met1–Thr40, Pro46–Asn58, and Glu75–Lys96 are disordered, partially overlapping with those predicted by VL-XT. However, IUPRED (Figure 2A, top panel, green line) predicts that the protein is ordered, as does the charge hydrophobicity phase-space analysis of PONDR (Figure 2C), although in the latter predictor, the protein (green diamond) is close to the frontier separating the space of ordered and disordered proteins. Then, the majority of the theoretical predictions suggest the presence of ordered structure mainly at the N-terminus (residues 1–70), which could account for the residual ellipticity observed in the far-UV CD (Figure 1A). However, except for the IUPRED (Figure 2A, top panel, green line), the rest of the servers predict the presence of disordered regions through the sequence of the protein.

Taken together, the experimental and theoretical approaches indicate that IF17 is an IDP with residual secondary structure and lack of a well-folded core.

**IF17N/IF7 Chimera Protein Is Also Disordered in Aqueous Solution.** Since (i) there is a sequence similarity between the full IF7 and C terminus of IF17,<sup>5</sup> (ii) both IF7 and IF17 have different stability against proteolysis,<sup>8</sup> and (iii) most of the theoretical predictions (see above) showed that the N-terminus of IF17 is, to a certain extent, ordered (Figure 2A,

top), we used a chimera protein (IF17N/IF7) formed by the 82 first residues of IF17 fused to IF7 to address (i) whether the fusion of both proteins resulted in a fully folded protein, which had a larger stability than the two separated proteins, and (ii) whether IF17N/IF7 was able to bind GS with a larger affinity than the wild-type proteins.

The fluorescence spectrum of IF17N/IF7 showed a maximum at 354 nm, due to the sole tryptophan in the sequence (from IF7); that wavelength indicates that the tryptophan is fully solvent-exposed, as in IF7.<sup>11</sup> The far-UV CD spectrum of IF17N/IF7 showed a similar shape to that of IF17, with a minimum at 200 nm and a shoulder at 222 nm (Figure 1A). The ellipticity at 222 nm was  $-5500 \text{ deg cm}^2 \text{ dmol}^{-1}$  which leads to a 14% of helical or turn-like structures. The chemical (Figure 1B) and thermal (Figure 1C) denaturations of IF17N/IF7 showed a similar behavior to those of IF17. Finally, the 1D NMR spectrum did not show dispersion in the amide, aromatic, and methyl regions; furthermore, the highly broad indole proton of the tryptophan appeared at 10.16 ppm, close to the expected value for random-coil polypeptides (10.22 ppm<sup>36</sup>) (Figure 1D), and the  $D$  of IF17N/IF7 was  $(7.4 \pm 0.8) \times 10^{-7} \text{ cm}^2 \text{ s}^{-1}$ , similar to that of IF17.

Theoretical predictions by using VL-XT indicate that most of the polypeptide chain is ordered: only residues Tyr33–Arg37 (also present in IF17), Ala77–Gln87, Ser108–Val116, and Thr136–Ser146 appeared disordered (Figure 2A, bottom panel, red line). Furthermore, the CDF analysis of PONDR predicts that IF17N/IF7 is a well-ordered protein (Figure 2A of Supporting Information). The RONN server predicts that the disordered patches are Ala70–Ser108 and Thr124–Ser146, that is, most of the IF7 chain of the IF17N/IF7 (Figure 2A, bottom panel, blue line). The FoldIndex server indicates that the polypeptide patches Met1–Thr40, Pro46–Asn58 (also present in IF17), Glu75–Arg89, and Gln103–Ser146 were disordered; it is interesting to note that those polypeptide regions partially overlapped with those predicted by VL-XT and RONN. Conversely, IUPRED predicts that IF17N/IF7 is ordered, except for residues Thr136–Ser146 (Figure 2A, bottom panel, green line), and the charge hydrophobicity phase-space analysis of PONDR (Figure 2B of Supporting Information) suggests that IF17N/IF7 is on the borderline separating the region of ordered and disordered proteins.

Thus, from the above experimental and theoretical results, IF17N/IF7 is an IDP, with a small percentage of secondary structure (Figure 1A).

**IF17 and IF17N/IF7 Bind to GS with Micromolar Affinity.** We have observed that IF7 folds upon binding to GS.<sup>11</sup> Then, we wondered whether IF17 also folds upon binding to GS. Furthermore, we were interested in determining if IF17N/IF7 (formed by proteins from *Synechocystis*) had more affinity for GS than the two isolated proteins. Trying to answer these questions, we monitored the binding of GS to both proteins by using a two-part approach. We first determined qualitatively the binding by steady-state far-UV CD and thermal denaturations followed by fluorescence and far-UV CD spectra. And second, we determined the apparent  $K_D$  by using fluorescence, as it has been reported in IF7,<sup>11</sup> and by far-UV CD.

The far-UV CD spectrum of GS was typical of an  $\alpha$ -helical protein, with intense minima at 222 and 208 nm.<sup>11</sup> The addition spectrum obtained by the sum of the spectra of isolated GS and IF17 was different from that of the complex

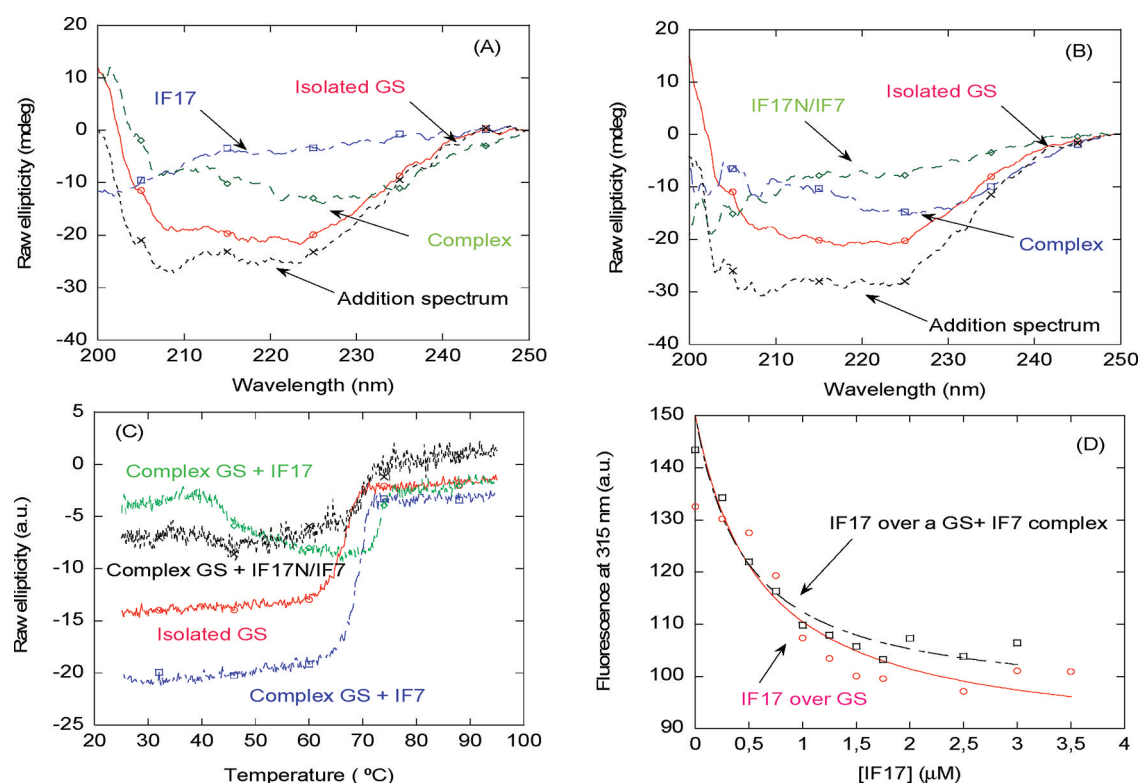


**Figure 3.** Binding between GS and IFs as monitored by biophysical and spectroscopic probes. (A) Far-UV CD spectra of the complex GS-IF17, of isolated GS, isolated IF17, and the resulting one from the addition of the spectra of isolated IF17 and GS. (B) Far-UV CD spectra of the complex GS-IF17N/IF7, of isolated IF17N/IF7, isolated GS, and the resulting one from the addition of the spectra of isolated IF17N/IF7 and GS. (C) Thermal denaturations followed by the changes in ellipticity at 222 nm, for the GS and the complexes GS-IF17, GS-IF17N/IF7, and GS-IF7. The y-axis scale is arbitrary: it has been modified to allow for the comparison among the traces of the thermograms. (D) Titrations to measure the apparent affinity of IF17 toward GS (1.5  $\mu\text{M}$ ) (red line, blank red circles) and that of IF17 toward a mixture composed of GS (1.5  $\mu\text{M}$ ) and IF7 (4  $\mu\text{M}$ ) (dot-and-dashed black line, blank black squares). The lines are the fittings to eq 1. All measurements were carried out at 25 °C in 10 mM phosphate buffer (pH 7.0).

(Figure 3A), thus indicating that there was binding; the same was observed in IF17N/IF7 (Figure 3B). Then, upon binding of GS to IFs, there is a change in the secondary structure of at least one, if not both, of the two proteins; it is tempting to suggest that IF17 and IF17N/IF7 alter their structures upon binding due to their smaller sizes and because they are IDPs. However, we cannot rule out, based on our data, conformational rearrangements in GS (see below). It is interesting to note that upon binding of IF17 (whether or not IF7 is present) there is a decrease (in absolute value) in the intensity of the spectra of the complex (instead of the expected increase) (Figure 3A,C of Supporting Information). Conversely, when IF7 is added to the solution, there is an increase (in absolute value) in the intensity of the difference spectra at 222 nm (and any other wavelength) as the concentration of IF7 is raised (Figure 3D of Supporting Information). Probably, there is a tendency of the IF17 to acquire  $\beta$ -sheet structure upon binding to GS and that a large addition of IF17 led to aggregation. In fact, we observed that over 5 h at 25 °C the titrating mixtures containing the complexes having an [IF17]  $\sim$ 1.5 times larger than the [GS] precipitated. This precipitation was slower, but still present, when the samples were incubated at 5 °C; thus, the samples for the binding titration experiments were prepared and measured within the next 3 h. These results agree with functional assays, since it has been shown that the complete inactivation of GS occurs at concentrations of IFs 4 times larger than the [GS].<sup>5</sup>

To further confirm binding, we carried out thermal denaturations of GS in the absence and in the presence of the IFs. Binding can be detected by a change in the thermal denaturation midpoint,  $T_m$ , of the complex, when compared to that of the isolated GS:<sup>41–43</sup> an increase of the  $T_m$  indicates binding of the corresponding IF to the folded state of GS; a decrease of the  $T_m$  indicates binding to the unfolded state of GS and/or complex destabilization due to conformational changes. In all the GS–IFs mixtures we observed an increase in the  $T_m$  of the complex, either followed by fluorescence or CD (Table 1 and Figure 3C). However, whereas the fluorescence thermograms showed a single sigmoidal transition when any of the IFs were added (at  $\sim$ 67 °C), the CD thermograms showed two transitions only when IF17 was present (at  $\sim$ 44 and  $\sim$ 67 °C); furthermore, the  $T_m$  of the transition at  $\sim$ 44 °C was IF17 concentration independent (from 1 to 3  $\mu\text{M}$ , Figure 3B of Supporting Information).

Next, we tried to determine quantitatively the  $K_D$  of the binding between GS and the IFs by using fluorescence (Figure 3) and CD (Figure 3 of Supporting Information). We observed that the  $K_D$ s determined by CD are similar, but not identical, to those determined by fluorescence (Table 2). There are two possible explanations for this behavior. First, subtracting the spectra of IFs at different concentrations from those of the complexes yielded to experimental data scattering (Figure 3C,D of Supporting Information) and, then, to poorer fittings; in most of the fluorescence curves, we did not have to subtract a



blank to the mixture of the complex due to the absence of tryptophan residues in IF17. Then, in this case, the differences between both values are due to the inherent imprecision of the technique. And second, in the CD titrations, we are subtracting the blank containing the corresponding isolated IFs, and then, we assume that there are not large structural changes in the GS-bound IFs, which could obscure the CD signal from the nonbound protein in excess. Besides, we are assuming that (i) no large structural changes occurred in GS upon IF7 binding and (ii) when the other IF is already present and bound to GS, it does not experience any conformational change to allow for binding of the other IF. Since in fluorescence we are monitoring the nearby environment around tryptophan or tyrosine residues, this technique cannot map structural changes which are not affecting those fluorescence residues. Thus, under this scenario, the apparent  $K_D$  determined by CD would be monitoring binding and conformational rearrangements (in the corresponding IF and/or in GS).

The apparent  $K_D$  of IF17 alone for GS, as determined by fluorescence, is slightly larger (1  $\mu$ M) than that of IF7 (0.3  $\mu$ M<sup>11</sup>) (Table 2 and Figure 3). We also attempted to elucidate the stoichiometry by using the procedure described by Otzen and co-workers.<sup>44</sup> In this approach, a plot of the difference between the measured fluorescence of the complex, and that expected from the contribution of the individual protein components, versus the ratio [titrating IF protein]/[GS protomer] provides two straight lines whose intersection gives the stoichiometry of the complex studied; the errors in the intersection coordinate were estimated from the fitting errors in the slopes and the  $y$ -axis intersections of both lines. Then, in the GS–IF system, although the stoichiometries seem to be slightly different (0.5 versus 1), giving the large errors, we cannot be certain whether the values change among the different GS–IF complexes formed. We did not attempt to determine the stoichiometries from the CD data due to the worse signal-to-noise ratio of the obtained difference spectra.

## DISCUSSION

**IF17 Is an IDP.** The results show that IF17 is an IDP, with neither stable hydrogen bonds nor a well-formed core. To the best of our knowledge, this is the first report on the conformational stability and structure of an IF17-like inactivating factor.

The lack of dispersion of the amide signals in the NMR spectrum (Figure 2D) and the absence of cooperativity during the thermal and chemical denaturations (followed by CD and/or fluorescence) also support that the tertiary structure of IF17, if any, is very weak and no hydrophobic core is formed. Most of the theoretical results also support that IF17 is disordered in several regions (Figure 2). There was, however, evidence of a small amount of ordered structure (~15%), as judged by the shoulder at 222 nm in the far-UV CD spectrum, which disappears at high denaturant concentrations (Figure 1B). This residual structure is not stably hydrogen-bonded, as shown by the hydrogen-exchange experiments. Furthermore, IF17 does not bind ANS (a probe used to detect partially folded states), suggesting that either the residual secondary structure in IF17 is not solvent-exposed or, alternatively, it does not involve a large amount of nearby hydrophobic residues (that is, the protein has not a compact hydrophobic core formed, as it is also shown in other IDPs<sup>45</sup>). We do not know the exact nature of that secondary structure in IF17, but it could involve an equilibrium between transient  $\alpha$ -helices, turn-like or PPII helical structures.

Interestingly enough, PPII conformations have been linked to protein–protein interactions<sup>46</sup> and to stabilization of sequences against conformational transformation.<sup>47</sup> We performed predictions to test for possible protein-binding sites of IF17 to GS by using the ANCHOR web server. In IF17, no binding sites were predicted (Figure 2A, top panel), but IF7 was predicted to have two binding regions, namely, Ala9–Lys19 and Leu26–Gly34, appearing the former also in the prediction of IF17N/IF7 (Figure 2A, bottom panel); however, it is important to keep in mind that because linear motifs are short in length, they contain very little information, and the prediction of binding sites from sequence alone has a high false positive rates.

Being IF17 an IDP offers entropic advantages, for the disorder-to-order transition that we have suggested should occur upon binding to GS (Figure 3 of Supporting Information), since highly specific interactions would decrease the conformational entropy of the binding reaction.<sup>48–50</sup> On the other hand, it has been argued that a common trait among IDPs is binding promiscuity,<sup>31,33,50</sup> adopting different structures upon binding to several targets. To the best of our knowledge, no other partners, rather than GS, have been observed for IF17; in fact, control steady-state spectra and thermal denaturations followed by CD, in the presence of equimolar amounts of IF17 and IF7, indicated the absence of binding between both IFs. Furthermore, control far-UV CD experiments in the presence of 1 M  $\text{NH}_4\text{NO}_3$  suggested that ammonium alone was not able to induce structure in either IF17 or IF7.

IF7 is also an IDP,<sup>11</sup> which shows a high sequence similarity with the C terminus of IF17. This result suggests that this region of IF17 could be involved in the interaction with GS, and thus, it might be responsible for its GS-inactivating activity.<sup>5</sup> Furthermore, from studies *in vitro* with crude extracts,<sup>8</sup> the stabilities toward proteases of IF7 and IF17 are different, and then, we reasoned that the differences in protease stability could be due to the N-terminus of IF17. To further support our hypothesis, the majority of the disorder predictors suggested that most of the N-terminal region of IF17 was ordered (Figure 2). Then, we used a chimera protein (IF17N/IF7) formed by the N-terminus of IF17 fused to the rest of IF7; our results show that the IF17N/IF7 was also an IDP, with a similar amount of residual structure as IF17 and IF7 (Figure 1A). That is, the higher stability of IF17 against proteolysis in crude extracts *in vitro* does not seem to be confined only to its N-terminus.

The IF17N/IF7 is the first reported chimera protein resulting from the fusion of two IDPs. Recently, Longhi and co-workers<sup>51</sup> have shown how disorder can influence order and vice versa by designing chimeras formed by IDPs fused to the GFP. Their results show that the overall structure, compactness, and stability of the chimera proteins all differ from what could be expected from the structural features of the isolated IDPs and GFP, probably due to interactions between the two fused domains. Here, we have shown that fusion of two IDPs, involved in the same inactivation process, leads to an IDP with the same residual structure as the two isolated domains.

**Binding of IF17 to GS: Structure.** In this work, we have shown that IF17 was able to bind GS by using steady-state and thermal denaturations followed by CD. However, the transitions were in all cases irreversible, as shown by precipitation of the sample after heating, and then a reliable thermodynamic interpretation on the relative stability of the complexes was not possible. The thermal denaturations of the GS complexes followed by CD in the presence of IF17

(whether or not IF7 is present) suggested the presence of an additional thermal transition (at  $\sim 44^\circ\text{C}$ ), which was not observed in GS–IF7 complex. This transition was not IF7 concentration dependent (Figure 3B of Supporting Information), and the change in the intensity of this transition (when compared to that of GS) was raised as the concentration of IF17 was increased; then, we suggest that such a transition is associated with the presence of IF17. Since the CD thermal unfolding of isolated IF17 did not show a sigmoidal transition (Figure 1C), these data indicate that upon binding to GS IF17 becomes, at least, partially folded (supporting our previous hypothesis based on the steady-state far-UV CD data, Figure 3A). Furthermore, the fact that the low-temperature transition is also observed in IF17N/IF7 implies that the folded region of “GS-bound”-IF17 involves its first 82 amino acids. Thus, not only the C-terminal region of IF17 seems to be important for binding (as suggested on grounds of sequence similarity<sup>5</sup>) but also its N-terminus. However, at the moment, we cannot rule out that the low-temperature transition observed could be associated with partial unfolding of GS or even aggregation of the IF17 N-terminal region (since no reversibility was observed in this transition, see Experimental Procedures); notwithstanding these findings, the facts that the  $T_m$  is not IF17 concentration dependent (Figure 3B of Supporting Information) and aggregation involves self-association (and then, a shift in the  $T_m$ ) seem to favor the hypothesis that the low thermal denaturation involves unfolding of IF17.

The region of “GS-bound”-IF17, which unfolds upon heating, does not seem to be involved in the binding of GS at pH 8.5, since the low thermal transition was not observed at this pH (Table 1); furthermore, the stability of GS at this pH is smaller than at physiological pH as concluded from the lower  $T_m$  (Table 1). These findings agree with previous suggestions that the GS–IF17 complex was weakened at pH 8.5,<sup>10</sup> but not because the structure of IF17 is pH-dependent (Figure 1 of Supporting Information), but because there are variations in the protonation state of some GS residues. These variations should alter GS stability and result in changes of its catalytic activity.

**Binding of IF17 to GS: Affinity and Biological Implications.** At this stage, it is important to note that if the IFs adopt a partially folded conformation upon binding to GS, then the intrinsic binding constant,  $K_{D0}$ , must be larger than the apparent  $K_D$  estimated by fluorescence or CD (Table 2), which involves binding and folding. Then, the structural rearrangement is supposed to penalize the binding energetics, and if  $K = [\text{folded}]/[\text{unfolded}]$  is the conformational equilibrium constant for a conformational change coupled to ligand binding,  $K_D$  is given by  $K_{D0}/(1 + 1/K)$ .

The facts that (i) we can follow binding by fluorescence and (ii) IF17 has no tryptophan residues suggest that at least the environment of one of the tryptophans of GS is altered upon binding. The apparent  $K_D$  of the GS–IF17 complex was in the range of  $1\ \mu\text{M}$ . This value is slightly larger than that obtained for IF7 ( $0.3\ \mu\text{M}^{11}$ ), suggesting that the interaction of GS with IF17 is slightly weaker. This result did not agree with our previous findings,<sup>5</sup> since we have shown by using protein–protein band shift and cross-linking experiments that the complex GS–IF17 appeared over-represented. The discrepancy between both values could be due to (i) the fact that we have used techniques which allow a qualitative estimation of the GS–IFs affinity in the presence of external agents (a gel matrix

and a cross-linker, in 50 mM KCl of ionic strength) or (ii) even partial degradation of IF7 in our crude extracts.

It is interesting to note that upon binding, IF17 seems to fold, although the acquired structure is not very rigid (as judged by the low  $T_m$  observed, Table 1, Figure 3C, Figure 3B of Supporting Information). We hypothesize that formation of the GS–IF complexes (either IF7 or IF17) do not follow a rigid-body mechanism,<sup>52</sup> but rather the IF should have enough flexibility to form a loose overall assembly with either the isolated GS or the previously formed GS–IF complex; in that way, the IF could undergo different rounds of disorder–order transitions to strengthen the overall complex. The presence of this weakly structured (“fuzzy”) complex could explain several experimental findings. First, it could explain why the values of the apparent  $K_{DS}$  of the different GS–IF mixtures are similar (Table 2); the “fuzzy” complex should be tightened, and therefore, better regulated, by the presence of the other incorporated IF. Second, the presence of this “fuzzy” complex explain the partial reactivation of GS at pH 8.5, even though IF17 is still present in the bulk media, and IF7 has been degraded.<sup>8</sup> Third, it could account for the observed small differences in the  $K_D$  measured by fluorescence and CD (Table 2), since the equilibrium constants monitored by far-UV CD should be monitoring binding and structural rearrangements in the previously GS-bound-IF complex or even in GS. And finally, the presence of this weakly structured complex would also explain why IF17N/IF7 did not show a larger affinity for GS than the two isolated proteins (Table 2); in the absence of the C terminus of IF17, the complex GS–IF17N/IF7 is not fully formed, and probably it might be more weakly structured than that the GS–IF17 complex, given the difference in the  $T_m$ s for the GS–IF17 and GS–IF17/IFN complexes (Table 2). Thus, it seems that the weak formation of structure in the IFs upon binding to GS or in the GS–IF complexes, in the ternary GS–IFs system, is required to achieve a better and tighter regulation of the function of GS.

## ■ ASSOCIATED CONTENT

### ● Supporting Information

Three figures showing the pH titration of IF17 followed by far-UV CD experiments (Figure 1), the PONDR predictions for IF17N/IF7 (Figure 2), and selected CD binding titrations, with the thermal denaturations at different IF17 concentrations (Figure 3). This material is available free of charge via the Internet at <http://pubs.acs.org>.

## ■ AUTHOR INFORMATION

### Corresponding Author

\*Tel +34 954489573, Fax + 34 954460065, e-mail [imuro@ibvf.csic.es](mailto:imuro@ibvf.csic.es) (M.I.M.-P.); Tel + 34 966658459, Fax +34 966658758, e-mail [jlineira@umh.es](mailto:jlineira@umh.es) (J.L.N.).

### Author Contributions

<sup>†</sup>These two authors contributed equally to this work.

### Funding

This work was supported by the Spanish Ministerio de Ciencia e Innovación (MCINN) (SAF2008-05742-C02-01, CSD2008-00005 to J.L.N., and BFU2010-15708 with Fondo Social Europeo (FSF) to F.J.F.), Generalitat Valenciana (ACOMP2011/113 to J.L.N.), and Junta de Andalucía (BIO-284 to F.J.F.). C.V.G. and L.S. were recipients from fellowships of the MCINN (FPU and FPI fellowships, respectively).

## ACKNOWLEDGMENTS

We thank the three anonymous reviewers for helpful and stimulating suggestions and discussions. We deeply thank May García, María del Carmen Fuster, and Javier Casanova for technical assistance and Drs. Francisco N. Barrera and David Aguado-Llera for critical comments.

## ABBREVIATIONS

ANS, 1-anilino-8-naphthalenesulfonate; *D*, diffusion coefficient; CD, circular dichroism; CDF, cumulative distribution function; GOGAT, glutamate synthase; GdmCl, guanidinium hydrochloride; GFP, green fluorescent protein; GS, glutamine synthetase I from the cyanobacterium *Synechocystis* sp. PCC 6803; IDP, intrinsically disordered protein; IF, inactivating factor; IF7, the *Synechocystis* 65-residue-long IF of GS; IF7A, the IF7 protein from *Anabaena* sp. PCC 7120; IF17, the *Synechocystis* 149-residue-long IF of GS; IF17N/IF7, chimera protein formed by the first 82 residues from IF17 fused to IF7; *K<sub>d</sub>*, dissociation constant; NMR, nuclear magnetic resonance; ORF, open reading frame; PONDR, predictor of natural disordered regions; PPII, polyproline helix; *R*, hydrodynamic radius; TSP, sodium trimethylsilyl[2,2,3,3-<sup>2</sup>H<sub>4</sub>]propionate; *T<sub>m</sub>*, thermal denaturation midpoint (expressed in °C); UV, ultraviolet.

## REFERENCES

- (1) Leigh, J. A., and Dodsworth, J. A. (2007) Nitrogen regulation in bacteria and archaea. *Annu. Rev. Microbiol.* 61, 349–377.
- (2) Luque, I., and Forchhammer, K. A. (2008) Nitrogen assimilation and C/N balance sensing, in *The Cyanobacteria: Molecular Biology, Genetics and Evolution* (Herrero, A., and Flores, E., Eds.) pp 335–382, Caister Academic Press, Norwich, UK.
- (3) Muro-Pastor, M. I., Reyes, J. C., and Florencio, F. J. (2005) Ammonium assimilation in cyanobacteria. *Photosynth. Res.* 83, 135–150.
- (4) Reitzer, L. (2003) Nitrogen assimilation and global regulation in *Escherichia coli*. *Annu. Rev. Microbiol.* 57, 155–176.
- (5) García-Domínguez, M., Reyes, J. C., and Florencio, F. J. (1999) Glutamine synthetase inactivation by protein-protein interaction. *Proc. Natl. Acad. Sci. U. S. A.* 96, 7161–7166.
- (6) Reyes, J. C., and Florencio, F. J. (1995) A novel mechanism of glutamine synthetase inactivation by ammonium in the cyanobacterium *Synechocystis* sp. PCC 6803: involvement of an inactivating protein. *FEBS Lett.* 367, 45–48.
- (7) Galmozzi, C. V., Saelices, L., Florencio, F. J., and Muro-Pastor, M. I. (2010) Posttranscriptional regulation of glutamine synthetase in the filamentous cyanobacterium *Anabaena* sp. PCC 7120: differential expression between vegetative cells and heterocysts. *J. Bacteriol.* 192, 4701–4711.
- (8) Galmozzi, C. V., Fernández-Avila, M. J., Reyes, J. C., Florencio, F. J., and Muro-Pastor, M. I. (2007) The ammonium-inactivated cyanobacterial glutamine synthetase I is reactivated *in vivo* by a mechanism involving proteolytic removal of its inactivating factors. *Mol. Microbiol.* 65, 166–179.
- (9) García-Domínguez, M., Reyes, J. C., and Florencio, F. J. (2000) NtcA represses transcription of *glaA* and *glaB* genes that encode inhibitors of glutamine synthetase type I from *Synechocystis* sp. PCC 6803. *Mol. Microbiol.* 35, 1192–1201.
- (10) Herrero, A., Muro-Pastor, A. M., and Flores, E. (2001) Nitrogen control in cyanobacteria. *J. Bacteriol.* 183, 41–425.
- (11) Muro-Pastor, M. I., Barrera, F. N., Reyes, J. C., Florencio, F. J., and Neira, J. L. (2003) The inactivating factor of glutamine synthetase IF7 is a natively unfolded protein. *Protein Sci.* 12, 1443–1454.
- (12) Gill, S. C., and von Hippel, P. H. (1989) Calculation of protein extinction coefficients from amino acid sequence data. *Anal. Biochem.* 182, 319–326.
- (13) Czipionka, A., de los Paños, O. R., Mateu, M. G., Barrera, F. N., Hurtado-Gómez, E., Gómez, J., Vidal, M., and Neira, J. L. (2007) The isolated C-terminal domain of Ring1B is a dimer made of stable, well-structured monomers. *Biochemistry* 46, 12764–12776.
- (14) Benjwal, S., Verma, S., Röhm, K.-H., and Gursky, O. (2006) Monitoring protein aggregation during thermal unfolding in circular dichroism experiments. *Protein Sci.* 15, 635–639.
- (15) Piotto, M., Saudek, V., and Sklenar, V. (1992) Gradient-tailored excitation for single-quantum NMR spectroscopy of aqueous solutions. *J. Biomol. NMR* 2, 661–665.
- (16) Wilkins, D. K., Grimshaw, S. B., Receveur, V., Dobson, C. M., Jones, J. A., and Smith, L. J. (1999) Hydrodynamic radii of native and denatured proteins measured by pulse field gradient NMR techniques. *Biochemistry* 38, 16424–16431.
- (17) Li, X., Romero, P., Rani, M., Dunker, A. K., and Obradovic, Z. (1999) Predicting protein disorder for N-, C-, and internal regions. *Genome Inform.* 10, 30–40.
- (18) Romero, P., Obradovic, Z., Li, X., Garner, E., Brown, C., and Dunker, A. K. (2001) Sequence complexity of disordered proteins. *Proteins* 42, 38–48.
- (19) Dosztányi, Z., Csizsók, V., Tompa, P., and Simon, I. (2005) The pairwise energy content estimated from amino acid composition discriminates between folded and intrinsically unstructured proteins. *J. Mol. Biol.* 347, 827–839.
- (20) Dosztányi, Z., Csizsók, V., Tompa, P., and Simon, I. (2005) IUPred: web server for the prediction of intrinsically unstructured regions of proteins based on estimated energy content. *Bioinformatics* 21, 3433–3444.
- (21) Yang, Z. R., Thomson, R., McNeil, P., and Esnouf, R. M. (2005) RONN: the bio-basis function neural network technique applied to the detection of natively disordered regions in proteins. *Bioinformatics* 21, 3369–3376.
- (22) Prilusky, J., Felder, C. E., Zeev-Ben-Mordehai, T., Rydberg, E. H., Man, O., Beckmann, J. S., Silman, I., and Sussman, J. L. (2005) FoldIndex: a simple tool to predict whether a given protein sequence is intrinsically unfolded. *Bioinformatics* 21, 3435–3438.
- (23) Mészáros, B., Simon, I., and Dosztányi, Z. (2009) Prediction of protein binding regions in disordered proteins. *PLoS Comput. Biol.* 5, e1000376 DOI: .
- (24) Doztányi, Z., Mészáros, B., and Simon, I. (2009) ANCHOR: web server for predicting protein binding regions in disordered proteins. *Bioinformatics* 25, 2745–2746.
- (25) Schmid, F. X. (1997) Optical spectroscopy to characterize protein conformation and conformational changes, in *Protein Structure* (Creighton, T. E., Ed) 2nd ed., pp 261–297, Oxford University Press, Oxford, UK.
- (26) Woody, R. W. (1995) Circular dichroism. *Methods Enzymol.* 246, 34–71.
- (27) Kelly, S. M., and Price, N. C. (2000) The use of circular dichroism in the investigation of protein structure and function. *Curr. Protein Pept. Sci.* 1, 349–384.
- (28) Shi, Z., Woody, R. W., and Kallenbach, N. R. (2002) Is polyproline II a major backbone conformation in unfolded proteins? *Adv. Protein Chem.* 62, 163–240.
- (29) Whitmore, L., and Wallace, B. A. (2004) DICHROWEB, an online server for protein secondary structure analyses from circular dichroism spectroscopic data. *Nucleic Acids Res.* 32, W668–W673.
- (30) Whitmore, L., and Wallace, B. A. (2008) Protein secondary structure analyses from circular dichroism spectroscopy: methods and reference databases. *Biopolymers* 89, 392–400.
- (31) Uversky, V. N. (2009) Intrinsically disordered proteins and their environment: effects of strong denaturants, temperature, pH, counter ions, membranes, binding partners, osmolytes and macromolecular crowding. *Protein J.* 28, 308–325.
- (32) Zurdo, J., Sanz, J., González, C., Rico, M., and Ballesta, J. P. G. (1997) The exchangeable yeast ribosomal acidic protein YP2b shows characteristics of a partly folded state under physiological conditions. *Biochemistry* 36, 9625–9635.



- (33) Uversky, V. N., and Dunker, A. K. (2010) Understanding protein non-folding. *Biochim. Biophys. Acta* 1804, 1231–1264.
- (34) Encinar, J. A., Mallo, G. V., Mizyricki, C., Giono, L., González-Ros, J. M., Rico, M., Cánepa, E., Moreno, S., Neira, J. L., and Iovanna, J. L. (2001) Human p8 is a HMG-I/Y-like protein with DNA binding activity enhanced by phosphorylation. *J. Biol. Chem.* 276, 2742–2751.
- (35) Kjaergaard, M., Nørholm, A.-B., Heldus-Altenburger, R., Pedersen, S. F., Poulsen, F. M., and Kragelund, B. B. (2010) Temperature-dependent structural changes in intrinsically disordered proteins: formation of  $\alpha$ -helices or loss of polyproline II? *Protein Sci.* 19, 1555–1564.
- (36) Wüthrich, K. (1986) *NMR of Proteins and Nucleic Acids*, Wiley, New York.
- (37) Tcherkasskaya, O., Davidson, E. A., and Uversky, V. N. (2003) Biophysical constraints for protein structure prediction. *J. Proteom. Res.* 2, 37–42.
- (38) Bernardo, P., and Blackledge, M. (2010) A self-consistent description of the conformational behaviour of chemically denatured proteins from NMR and small angle scattering. *Biophys. J.* 97, 2383–2390.
- (39) Marsh, J. A., and Forman-Kay, J. D. (2010) Sequence determination of compaction in intrinsically disordered proteins. *Biophys. J.* 98, 2383–2390.
- (40) Wang, Z., Plaxco, K. W., and Makarov, D. E. (2007) Influence of local and residual structures on the scaling behaviour and dimensions of unfolded proteins. *Biopolymers* 86, 321–328.
- (41) Pantoliano, M. W., Petrella, E. C., Kwanoski, J. D., Lobanov, V. S., Myslik, J., Graf, E., Carver, T., Asel, E., Springer, A. R., Lane, P., and Salemme, F. R. (2001) High-density miniaturized thermal shift assays as a general strategy for drug discovery. *J. Biomol. Screening* 6, 429–440.
- (42) Waldron, T. T., and Murphy, K. P. (2003) Stabilization of proteins by ligand binding: application to drug screening and determination of unfolding energetics. *Biochemistry* 42, 5058–5064.
- (43) Layton, C. J., and Hellinga, H. W. (2010) Thermodynamic analysis of ligand-induced changes in protein thermal unfolding applied to high-throughput determination of ligand affinities with extrinsic fluorescent dyes. *Biochemistry* 49, 10831–1041.
- (44) Otzen, D. E., Lundvig, D. M. S., Wimmer, R., Nielsen, L. H., Pedersen, J. R., and Jensen, P. H. (2005) p25 $\alpha$  is flexible but natively folded and binds tubulin with oligomeric stoichiometry. *Protein Sci.* 14, 1396–1409.
- (45) Szasz, C., Alexa, A., Toth, K., Rakacs, M., Langowski, J., and Tompa, P. (2011) Protein disorder prevails under crowded conditions. *Biochemistry* 50, 5834–5844.
- (46) Cubellis, M. V., Caille, F., Blundell, T. L., and Novell, S. C. (2005) Properties of polyproline II, a secondary structure element implicated in protein-protein interactions. *Proteins* 58, 880–892.
- (47) Darnell, G., Orgel, J. P. R. O., Pahl, R., and Meredith, S. C. (2007) Flanking polyproline sequences inhibit  $\beta$ -sheet structure in polyglutamine segments by inducing PPII-like helix structure. *J. Mol. Biol.* 374, 688–704.
- (48) Receuver-Brechot, V., Bourhis, J. M., Uversky, V. N., Canard, B., and Longhi, S. (2006) Assessing protein disorder and induced folding. *Proteins* 62, 24–25.
- (49) Uversky, V. N. (2002) Natively unfolded proteins: a point where biology waits for physics. *Protein Sci.* 11, 739–756.
- (50) Tompa, P. (2002) Intrinsically unstructured proteins. *Trends Biochem. Sci.* 27, 527–533.
- (51) Samb, I., Gatti-Lafronconi, P., Longhi, S., and Lotti, M. (2010) How disorder influences order and viceversa-mutual effects in fusion proteins containing an intrinsically disordered and globular protein. *FEBS J.* 277, 4438–4451.
- (52) Tompa, P., and Fuxreiter, M. (2008) Fuzzy complexes: polymorphism and structural disorder in protein-protein interactions. *Trends Biochem. Sci.* 27, 527–533.
- (53) Hughes, I. G., and Hase-Thomas, P. A. (2010) *Measurements and Their Uncertainties: A Practical Guide to Modern Error Analysis*, Oxford University Press, Oxford, UK.